The 2015 World Congress on
Advances in Structural Engineering and Mechanics (ASEM15)
Incheon, Korea, August 25-29, 2015

Analytical Investigations on Seismic Responses of a 25-story RC Flat-Plate Core-Wall Building Structure

*Kyung Ran Hwang[1)] and Han Seon Lee[2)]

[1), 2)] *School of Civil, Environmental, and Architectural Engineering, Korea University, Seoul, 136-713, Korea*
[1)] dh8149@korea.ac.kr

ABSTRACT

The purpose of this study is to investigate the seismic responses of an RC high-rise flat-plate core-wall building structural system. For this purpose, an analytical model was calibrated with the results of the earthquake simulation tests on a 1:15 scale 25-story distorted model. This calibrated model was then transformed to a true model. Then, this transformed true model was subjected to series of earthquake ground motions to investigate the contribution of shear wall and columns with slabs and coupling beams. The foundation rocking tends to increase the lateral resistance of the flat-plate frame, and to decrease the inelastic energy dissipation of the core wall with the d demands on the moment and the curvature of the core wall than those of fixed-base model. Under the maximum considered earthquake (MCE) in Korea, the walls with special boundary elements in the first story did not exhibit any significant inelastic behavior with a maximum curvature being only 10~15% of the intended ultimate value of in the design phase, 0.041rad/m.

1. INTRODUCTION

Recently, the number of high-rise residential buildings (higher than 30 stories) has been increasing, for the efficient use of available housing sites in Korea. For these high-rise buildings, a combined system of core reinforced concrete (RC) shear walls: a lateral load resistance structural system, and RC flat plate frames: a gravity load resistance structural system, has been widely used. Representative flat-plate core-wall buildings constructed in Korea are shown in Fig. 1(a). This structural type is classified as dual frame or building frame systems in current seismic provisions, KBC 2009 (AIK, 2009) and IBC 2006 (ICC, 2006). For the shear walls in the building frame system, special shear walls, for which special seismic detailing requirements are imposed, or ordinary shear walls, which have a height restriction, have generally been used. However, in the case of the RC flat plate structure, seismic detailing requirements for

---

[1)] Graduate Student
[2)] Professor

the connection with columns are given only as part of intermediate moment frames. In the dual frame or building frame systems, two vertical shear walls commonly include regular openings, and are connected to each other with coupling beams, which have a great effect on the lateral resistance behavior. Although a number of experimental and analytical studies have been done on the high-rise structure, the information is still not sufficient for design of these building structures.

In this study, the seismic responses of an RC high-rise flat-plate core-wall building structural system are investigated by the analytical simulation of shake-table responses of a 1:15 scale 25-story flat-plate core-wall RC residential building model.

2. OUTLINE OF EXPERIMENTS

Among the RC flat-plate core-wall building structures constructed in Korea, the most typical type was chosen as a prototype: This was originally a 35-story flat-plate building, where each floor has four dwelling units, and each dwelling unit has the size of 188m^2, as shown in Fig. 1 (b). However, due to limitation in the capacity of the shake table at the Earthquake Simulation Test center of Pusan National University (size 5m x 5m, payload 600kN) and for the convenience of construction of the model, the number of the stories of the prototype for the shaking table test was reduced to 25 (height: 79.5m), and staircases and slabs inside the core walls were all omitted as shown in Fig. 1 (c). The height of the first story is 5.1m, with those of the other stories being 3.1m. In the prototype building, core walls were designed to take most of resistance to the lateral load, and peripheral frames are designed to resist only the gravity load, in accordance with the definition of the building frame system. The result of elastic analysis of the prototype building shows that the core walls resisted 87% of the total lateral load. The size of all the peripheral columns was determined as 900×900mm, and the thickness of the core walls is 600mm, with that of the slab being 300mm, all along the height of the structure. The design concrete strength (f'_c), 40 MPa, and the yield strength of reinforcement, 400MPa, are applied to the whole building structure. The dead load of the prototype is 12,257kN for the second floor, 10,340kN for the typical floors (third to twenty fifth floors), 10,960kN for the roof, and 261,000kN in total. The effective seismic weight is set as the dead load, and live load is not included.

The size and payload of a shaking table in the Earthquake Test Center of Pusan National University are 5m×5m and 600kN, respectively, and the model was scaled down to 1/15, taking availability of model reinforcement and constructability into consideration. Corresponding to the prototype reinforcement (D29, D16, D13) of the prototype, the scale model (1:15) used steel wires, ϕ2 and ϕ1 for model reinforcement. The average compressive strength of the model concrete is 46.9MPa, which is larger than design compressive strength, 40MPa. The average split tensile strength is 4.21MPa, about 1/10 of the compressive strength.

Even with a low reduction factor of 1/15, the required self-weight of the model is 1,160kN, which still exceeds the capacity of the shaking table, 600kN, if the true replica model were used. Therefore, the model's weight should be reduced further, by using a distorted model. Taking into account the length similitude factor, 1/15, and the weight of available steel plates for added artificial mass, the density similitude factor was chosen to be 4.18. Therefore, the acceleration similitude factor was determined as 3.59 to satisfy the similitude law. The total effective seismic weight of the prototype was

261,000kN (self-weight: 205,100kN, additional dead load: 55,900kN). According to the similitude law, the total effective seismic weight of the true replica model is 1,160kN (self-weight: 60.8kN, added load: 1,099kN), and the total weight of the test model, as for a distorted model, is 323kN, (self-weight: 60.8kN, added weight: 262.2kN) 1/3.59 of the total seismic weight of the true replica model. Detailed information on the design and construction of the specimen is given in the reference (Lee et al. 2015)

Fig. 2(a) shows an overview of the model. Displacement transducers and accelerometers were installed at the floors of the 6th, 10th, 14th, 18th, and 22nd stories, and at the roof, to measure the overall behavior of the model as shown in Fig. 2(c). Furthermore, displacement transducers were deployed to measure the local behaviors of the walls and foundations. The program of earthquake simulation tests is summarized in Table 1. The target or input accelerogram of the table was based on the recorded 1952 Taft N21E (X direction) and Taft S69E (Y-direction) components, and was formulated by compressing the time axis with the scale factor of, $1/\sqrt{3.59\times15}$, and by amplifying the acceleration with the scale factor, 3.59. X, Y, and XY in designation of each test mean that the excitations were implemented in the X direction only, in the Y direction only, and in the X and Y directions simultaneously, respectively.

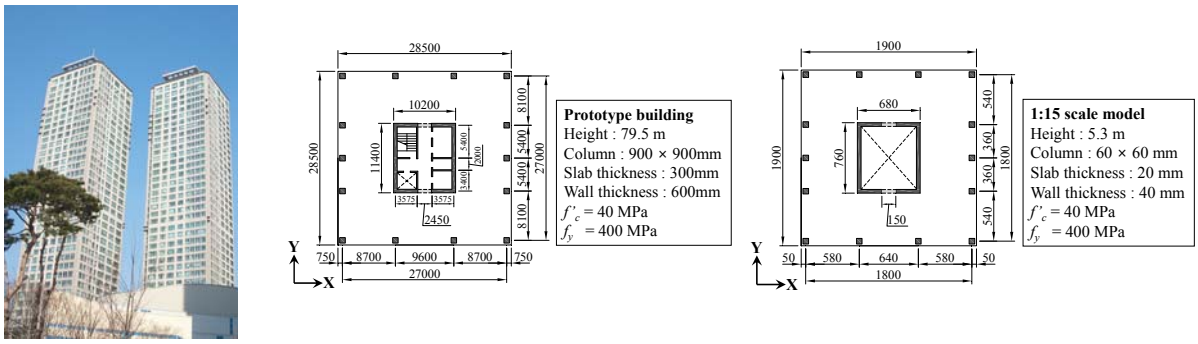

(a) Yongsan City Park in Seoul (35-story) (b) Plan of the prototype building (c) Plan of a 1:15 scale model

Fig. 1 Prototype building (unit: mm)

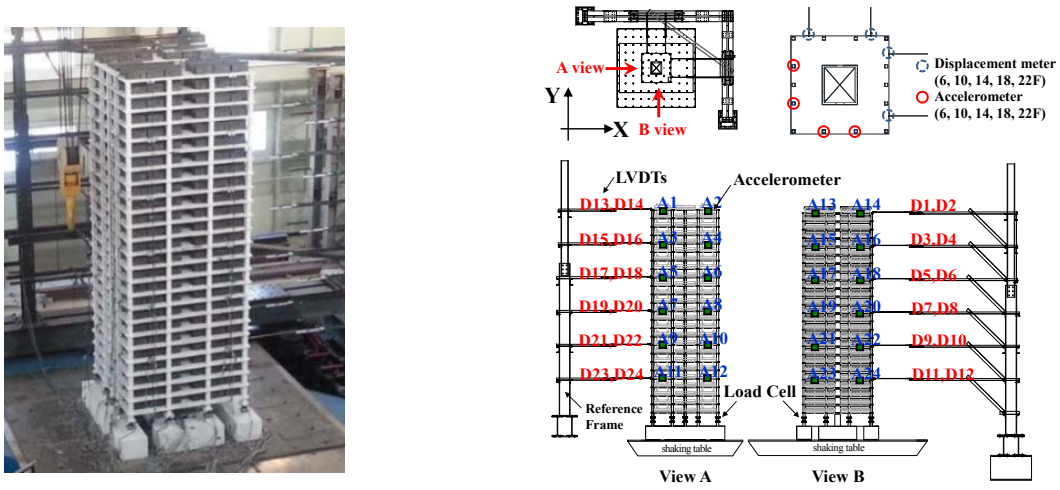

(a) Overview of the model (b) Instrumentation of the 1:15 scale model (D: disp., A: accel.)

Fig. 2 Experimental setup for earthquake simulation tests

Table 1. Test Program (X-dir.: Taft N21E, Y-dir.: Taft S69E)

Test Designation	Intended PGA(g)		Measured PGA(g) / 3.59		Return period in Korea	Test Designation	Intended PGA(g)		Measured PGA(g) / 3.59		Return period in Korea
	X-dir.	Y-dir.	X-dir.	Y-dir.			X-dir.	Y-dir.	X-dir.	Y-dir.	
White Noise (0.025 X, Y)						White Noise (0.025 X, Y)					
0.035X	0.035		0.0243		Elastic Behavior	0.187X	0.187		0.137		Design EQ. (DE)
0.035Y		0.040		0.034		0.187Y		0.216		0.167	
0.035XY	0.035	0.040	0.0243	0.034		0.187XY	0.187	0.216	0.137	0.167	
White Noise (0.025 X, Y)						White Noise (0.025 X, Y)					
0.07X	0.070		0.052		50 years	0.3X	0.300		0.226		MCE 2400 years
0.07Y		0.080		0.065		0.3Y		0.345		0.253	
0.07XY	0.070	0.080	0.052	0.065		0.3XY	0.300	0.345	0.226	0.253	
White Noise (0.025 X, Y)						White Noise (0.025 X, Y)					
0.154X	0.154		0.127		500 years	0.4X	0.400		0.300		DE in San Francisco USA
0.154Y		0.176		0.140		0.4Y		0.460		0.354	
0.154XY	0.154	0.176	0.127	0.140		0.4XY	0.400	0.460	0.300	0.354	

3. ANALYTICAL MODELING

Relationships between stress and strain for concrete and steel are given in Figs. 3(a) and (b). The material model of concrete (Fig. 3(a)) is “Todeschini model”, which could describe the cracking and crushing behavior of the concrete material with a nonlinear inelastic relationship. Since the envelope curve provided in PERFORM-3D cannot accept this model directly, the concrete curve is approximated with tri-linear line. Fig. 3(b) shows the material model of the reinforced bar, ϕ2. Specific material properties of concrete and reinforcement obtained in experiment are applied in analyses. The backbone curve between shear stress and strain for the concrete shear of wall is given in Fig. 3(c) according to ASCE/SEI 41-13 (2014). Walls are modeled as inelastic “Shear Wall” element, which has 4 nodes and 24 degrees of freedom. In the longitudinal direction of the element, the axial and in-plane bending behaviors are described by using the inelastic fiber sections as shown in Fig. 4(b), and the shear behavior is defined as the thickness of walls assigned to the inelastic concrete shear material in Fig. 3(c). Transverse in-plane bending is assumed to be elastic. Because the PERFORM-3D provides only an elastic slab model, slabs are composed of the inelastic beam elements with inelastic moment-curvature hinges obtained by inelastic sectional analyses, which can describe the contribution of the slabs to the lateral strength of the building and the out-of-plane behaviors. The width of the slabs is determined as shown in Fig. 4 (c) according to PEER/ATC 72-1 (2010). In addition, their diaphragm action for the rigid body motion is assumed. Coupling beams are modeled by using inelastic moment-curvature hinges at the ends of the beam. In order to take into account the influence of load cells beneath the footing, footings and load cells are modeled as the beam-column element. The result of shake table tests shows that the load cells were not rigidly connected to the footing. To reflect this phenomenon, the calibration for the analytical model was conducted by adjusting the values of axial stiffness of the elements for load cells.

Overview of the analytical model are given in Fig. 4(a). Gravity load analysis was conducted before nonlinear dynamic time history analysis. During 879 seconds of earthquake motion initiating from Taft 0.035g and up to Taft 0.4g as shown in Table 1 and Figs. 5 (a) and (b), the model was analyzed through the step-by-step procedure.

The acceleration was amplified with the scale factor, 3.59. Each base input excitation is the same as the output of table motion in each test and separated with neighbor input sufficiently so that there would be no inertial forces when a new round of analysis begins. However, since the analysis is continuously conducted for the whole series of input motions, the damage caused by the preceding run could be taken into account in the subsequent run of analysis. Time step is determined as 0.0039 seconds and output is obtained for every four steps in order to avoid excessive amounts of data.

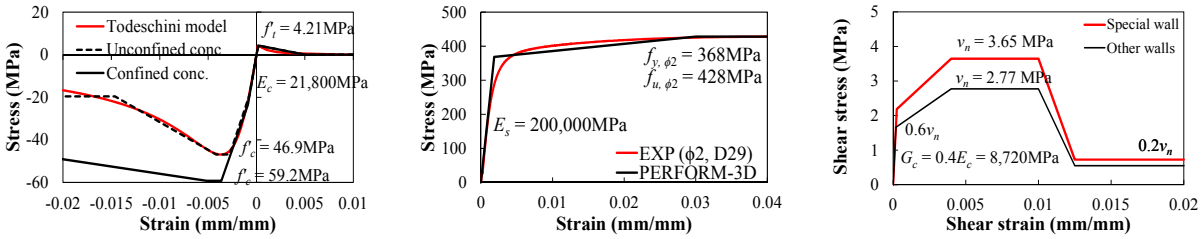

(a) Concrete (b) Steel (c) Shear material for wall

Fig. 3 Stress-strain relation of material

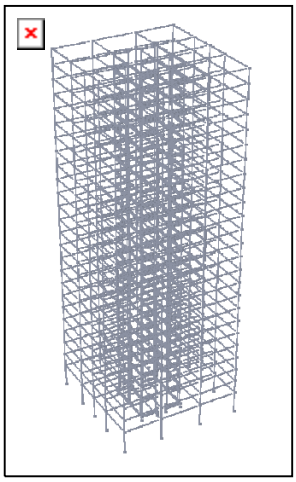

(a) Analysis model

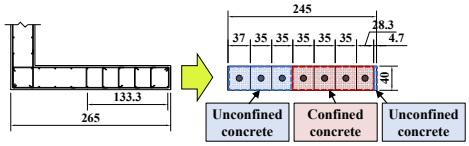

(b) Fiber section of the core wall

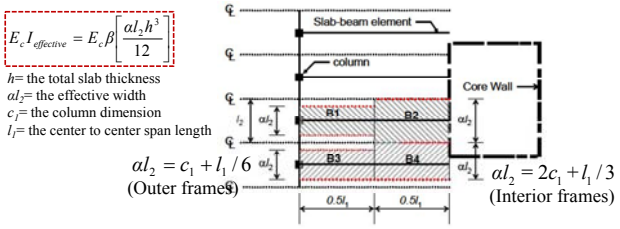

(c) Effective flexural stiffness of the slab (PEER/ATC 72-1)

Fig. 4 Details of modeling (unit: mm)

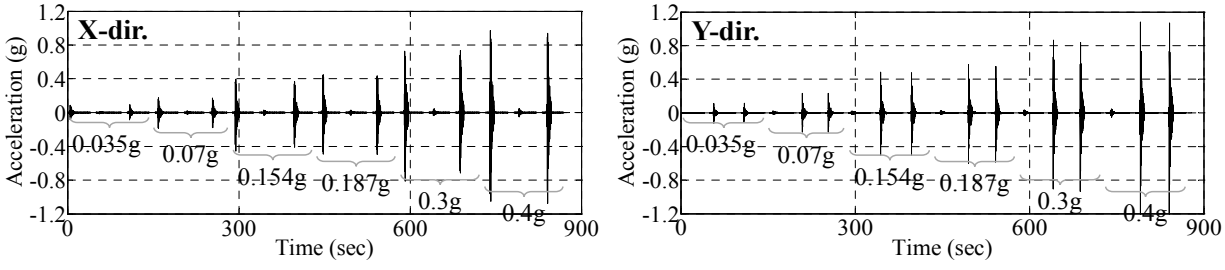

(a) X-dir. (b) Y-dir.

Fig. 5 Recorded table excitations used for analysis of distorted model (See Table 1)

4. CALIBRATION OF ANALYTICAL MODEL

The experimental and analytical time histories of the base shear coefficient (base shear/building weight, *V*/*W*) and the roof drift in the X and Y directions under the maximum considered earthquake (MCE), 0.3XY are compared in Fig. 6. The time history can be divided into the duration of table excitation, and that of no table excitation. No table excitation means the duration when free vibration occurs, after the shake table excitation was terminated. It can be noted that the maximum response of the base shear and roof displacement during the free vibration period reveals a level of maximum response similar to that during table excitation. The analytical model simulates well the time histories of the experiment during not only table excitation but also no excitation. In the test results, the rotation at the foundation due to the uplift of the foundation base are considerably large. In order to take into account the influence of load cells beneath the footing, footings and load cells are modeled as the elastic beam-column element. The axial stiffness of the load cell was calibrated by matching the fundamental periods and the axial deformation of the footing. Fig. 7 shows that the experimental and analytical time histories of the axial deformations at the edge of the footing, RF1 and RF2. The analytical model simulates well the foundation rocking of the experiment.

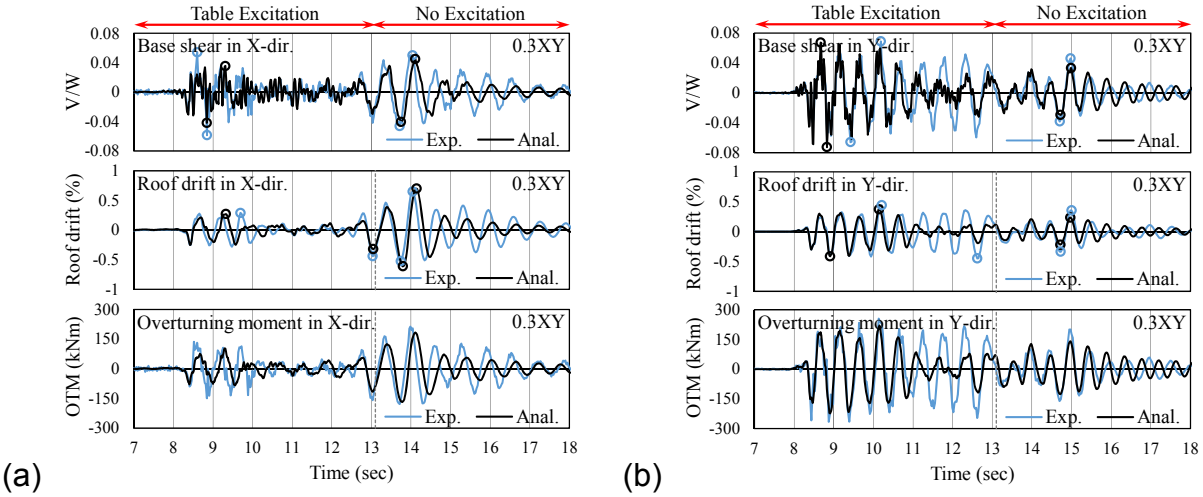

Fig. 6 Experimental and analytical relations of time history responses of base shear, roof drift, and overturning moment under 0.3XY(MCE, distorted model): (a)X-dir. and (b) Y-dir.

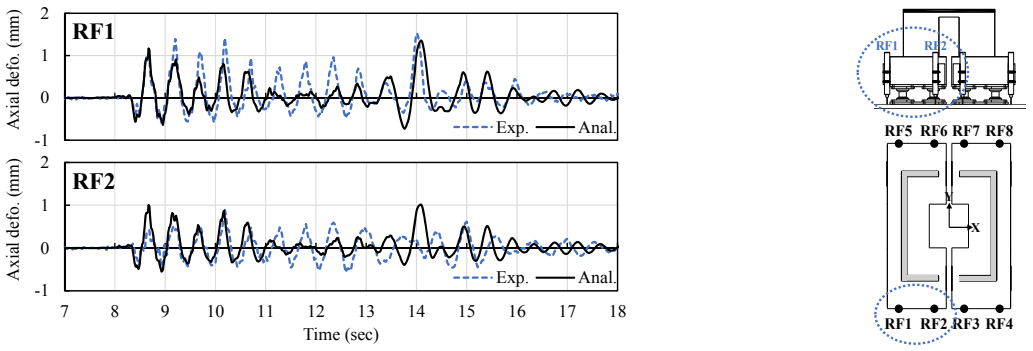

Fig. 7 Experimental and analytical relations of time history responses of axial deformation of the footing (distorted model)

The hysteretic curves between the base shear and the roof drift in the X- and Y-directions under 0.187XY, and 0.3XY are given in Fig. 8. Under 0.187XY (Fig. 8(a)), a low level of inelastic response is revealed in the hysteresis between the base shear and the drift in X- and Y-directions. Significant inelastic behaviors could be noticed in the hysteresis under 0.3XY (Fig. 8(b)). The analytical force-drift relations generally simulate well those of the experimental. However, in the hysteretic curve in X-direction under 0.3XY, the energy dissipation and strength of the analytical model underestimate those of experimental results. In case of the true replica model, the Y-directional behaviors are comparable to those of distorted model, but the maximum strength and the inelastic energy dissipation in the X-directional behavior under 0.3XY and 0.4XY are smaller than those of distorted model. Nevertheless, in general the differences between the true and distorted analytical models appear to be minor. *This paper presents only the seismic responses of the true replica model in the following analytical study.*

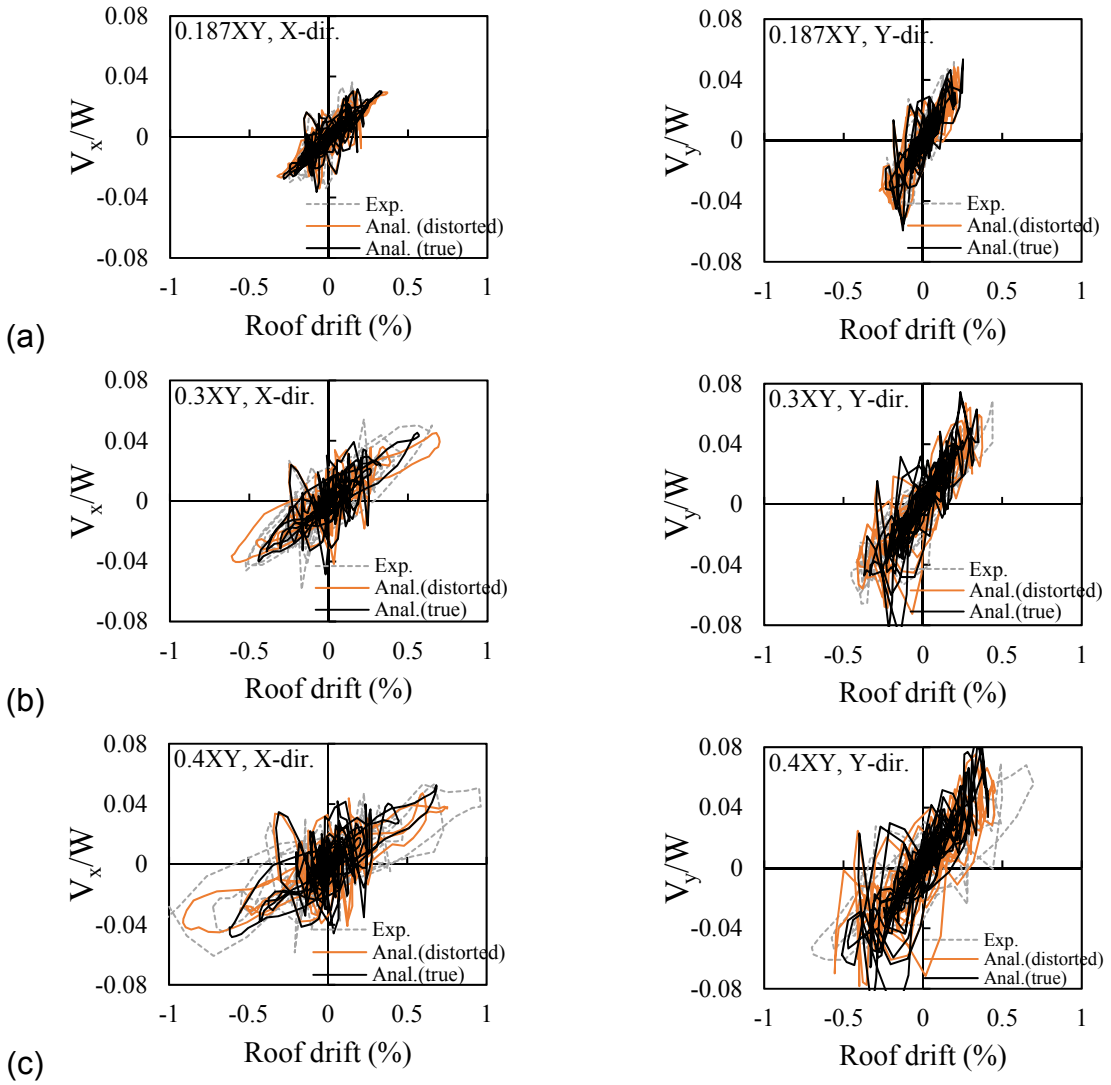

Fig. 8 Experimental and analytical relations of hysteretic curves between base shear coefficient (V/W) and roof drift: (a) 0.187XY (DE), (b) 0.3XY (MCE), and (c) 0.4XY

5. ANALYTICAL INVESTIGATIONS ON THE SEISMIC PERFORMANCE

5.1 Vertical distribution of shear force and moment

Fig. 9 reveals the vertical distributions of story shear resisted by the core-wall and flat-plate frame systems, respectively, at the instants of roof acceleration during table excitation and during no excitation. The distributions during table excitation reveals clearly that the higher modes governed in both of the X and Y directions, whereas those during no excitation were governed by the first mode. The distributions of the analysis (Fig. 9(a)) is similar to those of the experiment (Lee et al. 2015), and the higher mode effect could be simulated well.

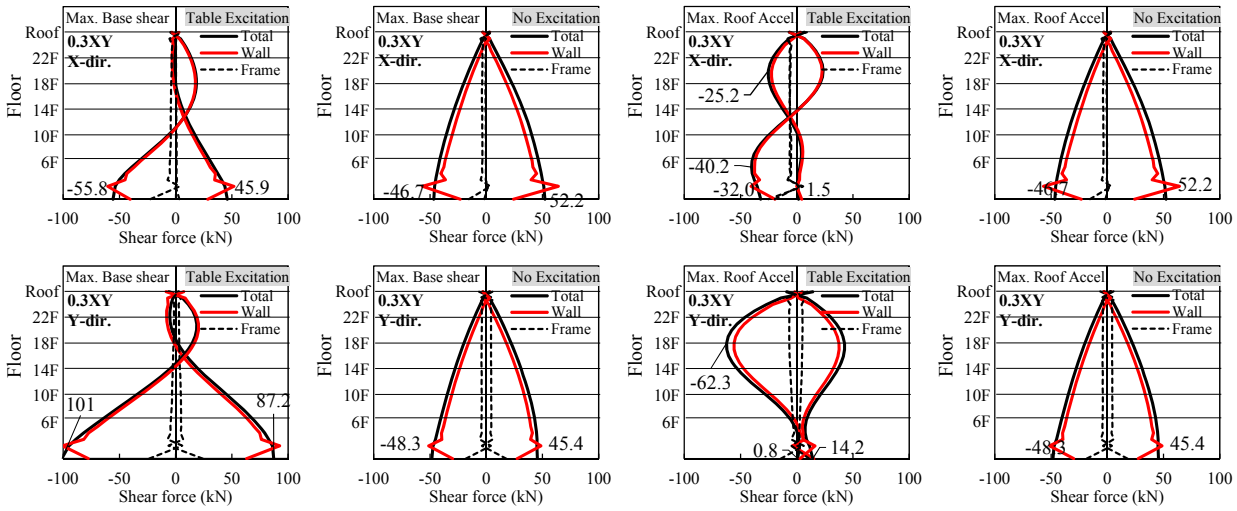

i) Instants of maximum base shear ii) Instants of maximum roof acceleration

(a) Flexible-base model

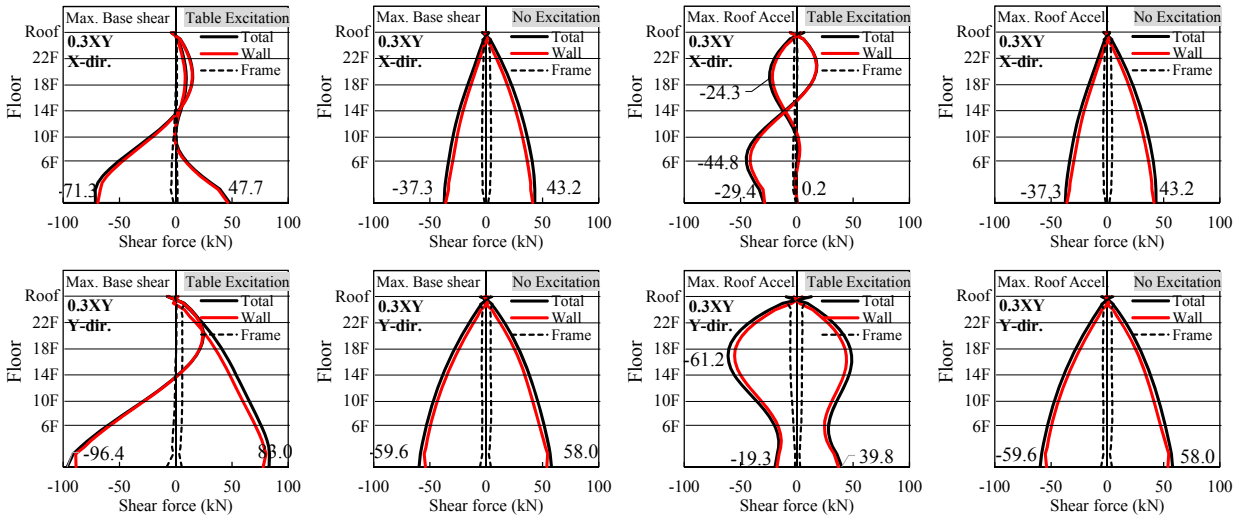

i) Instants of maximum base shear ii) Instants of maximum roof acceleration

(b) Fixed-base model

Fig. 9 Vertical distribution of story shear at instants of maximum base shear and roof acceleration

Models with either the foundation rocking (flexible base) or fixed base were used to evaluate the effect of base flexibility on the seismic response of the building model. The distributions of the total story shear (black-solid line) in the flexible-base model (Fig. 9(a)) are similar to those in the fixed-base model. During table excitation, the maximum values of story shear in the Y direction (flexible base: 62.3kN and fixed base: 61.2kN) occurred at the 18th story, and those are approximately 65% of the maximum base shear in Y direction (flexible base: 101kN and fixed base: 61.2kN). Over 90% of the story shear is resisted by the core-wall system. However, the shapes of the story shear below the 3rd floor in the flexible-base model are different to those in the fixed-base model, and the base shear contributed by the flat-plate frame is approximately 30~40%.

Fig. 10 shows the time history of the X-directional overturning moment (OTM) under MCE in Korea. In the flexible-base model (Fig. 10(a)), the maximum OTM due to tension/compression of coupling force (*Tl*: 69.6kNm) is approximately 58% of the OTM resisted by the core wall (M_{wall} = M_{w1} (left wall) + M_{w2} (right wall) + *Tl* = 120kNm) with the coupling force in the fixed-base model being 66.5% of the OTM resisted by the core wall.

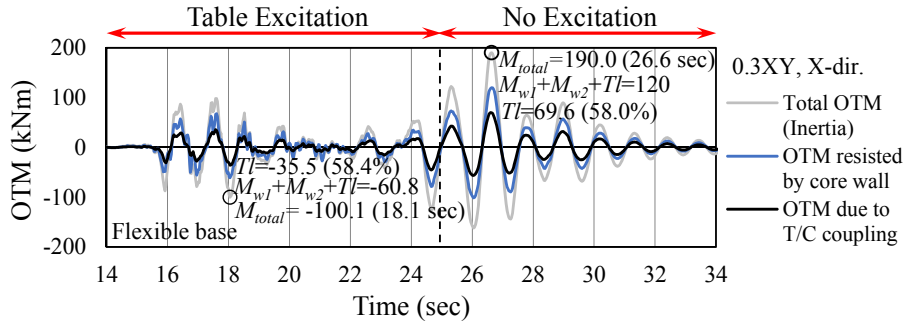

(a) Flexible base

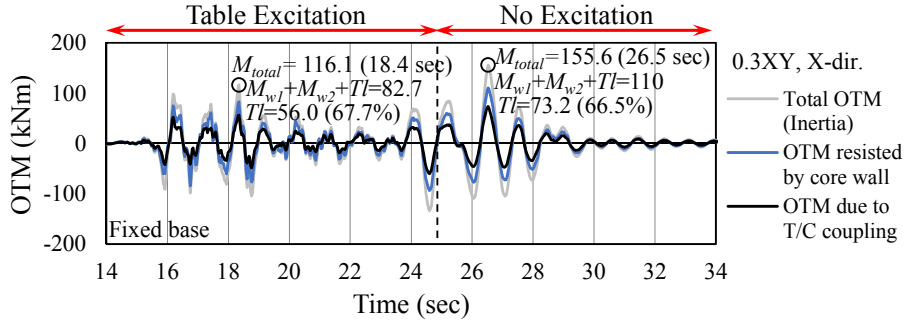

(b) Fixed base

Fig. 10 Time histories of overturning moment (OTM) contributed by tension/compression (T/C) coupling force under 0.3XY (MCE)

Fig. 11 compares the vertical distributions of X-directional story moments, M_{total}, M_{wall}, M_{frame}, *Tl*, M_{w1}, and M_{w2}, and shear force of the coupling beam, *V*, at the time instants of maximum roof acceleration during table excitation and during no excitation. At time instant 16.9 sec in the flexible-base model (Fig. 11(a)), the moment distribution of the core wall reveals that the higher modes govern, while that of the flat-plate frame is distributed linearly. In the moment distribution of the core wall, M_{wall} = M_{w1} + M_{w2} + *Tl*,

the moment at the 12th story is 32.2kNm, comparable to that at the first story, 44.5kNm, and the M_{w1}, M_{w2}, and Tl are 6.8%, 9.6%, and 83.2% of M_{wall}, respectively. The shape of the shear force distribution of the coupling beam also reveal the higher mode effect, but it is different to that of story moment distribution of the core wall. The maximum value of shear force in the coupling beam occurred at the 24th floor. At time instant 26.0 sec in the flexible-base model (Fig. 11(a)), the moment distributions were governed by the first mode. The shear forces in the coupling beam largely occurred at the 6th to 15th stories. In the fixed-base model (Fig. 11(b)), the base moment resisted by the flat-plate frame is about 30% of total OTM, which is smaller than that in the flexible-base model, 40~50% of total OTM.

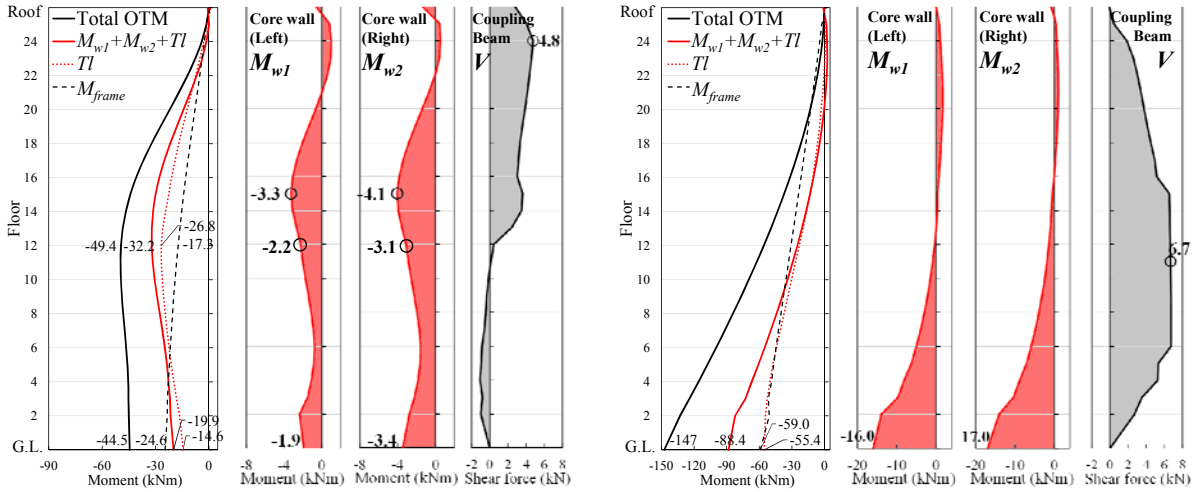

i) During table excitation, 16.9 sec ii) During no excitation, 26.0 sec

(a) Flexible-base model

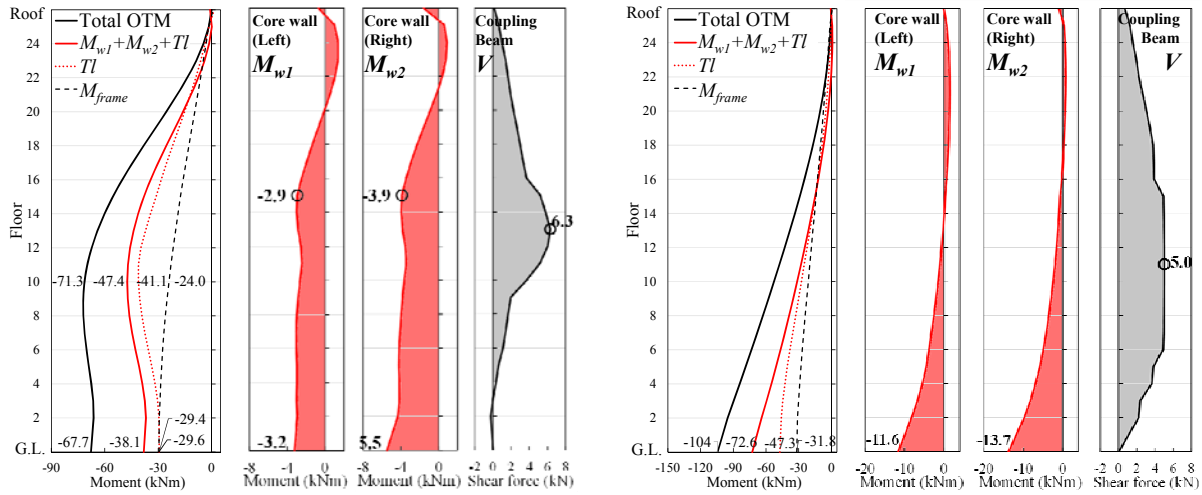

i) During table excitation, 18.7 sec ii) During no excitation, 27.1 sec

(b) Fixed-base model

Fig. 11 Vertical distribution of story moment at time instants of maximum roof acceleration

5.2 Energy dissipation

In the hysteretic curves between the base shear and roof drift (Fig. 8) under 0.3XY and 0.4XY, the significant energy dissipation is observed. Fig. 12 depicts time histories of the total dissipated energy, and Table 2 compares the amount of dissipated energy in each element group. In case of the flexible-base model, the amounts of the total dissipated inelastic energy under 0.187XY, 0.3XY, and 0.4XY are 375kNmm, 1,520kNmm, and 3,360kNmm, respectively. During the free vibration after termination of table excitation, 24.8s (0.3XY), the amount of dissipated inelastic energy increased greatly. Under 0.187XY, 60% of the total energy is dissipated by the coupling beam elements, whereas the ratio of the amounts of dissipated energy in the wall : coupling beam : slab is approximately 1:5:4 under 0.3XY.

The amount of the total dissipated energy in the fixed-base model is 90% of that in the flexible-base model. Under MCE in Korea, the ratio of the amounts of dissipated inelastic energy in the wall : coupling beam : slab in the fixed-base model is about 2:6:2. The fixed-base model increases the dissipated inelastic energy in the wall, while decreasing that in the slab, when compared with the case of the flexible-base model. Under MCE in Korea, the amount of the inelastic energy dissipated by the wall in the fixed-base model, 263kNmm, is significantly larger than that in the flexible-base model, 141kNmm, but the amount of the inelastic energy dissipated by the slab in the fixed-base model, 243kNmm, is less than that in the flexible-base model, 633kNmm.

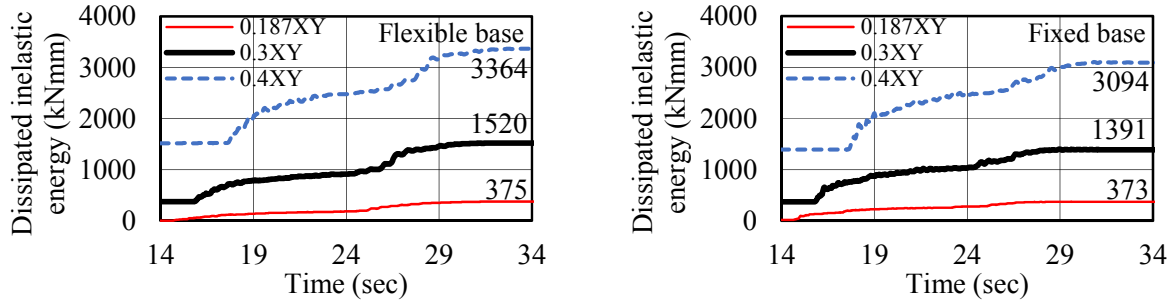

(a) Flexible-base model (b) Fixed-base model

Fig. 12 Dissipated inelastic energy

Table 2. Dissipated inelastic energy of element groups (unit: kNmm)

Element	(a) Flexible-base model			(b) Fixed-base model		
	0.187XY (DE)	0.3XY (MCE)	0.4XY (DE in S.F.)	0.187XY (DE)	0.3XY (MCE)	0.4XY (DE in S.F.)
Total	**375**	**1520**	**3364**	**373**	**1391**	**3094**
Core wall	15.8 (4.2%)	141 (9.3%)	387 (11.5%)	41.8 (11.2%)	263 (18.9%)	646 (20.9%)
Coupling beam	221 (58.9%)	745 (49.0%)	1518 (45.1%)	287 (77.1%)	886 (63.7%)	1834 (59.3%)
Slab	138 (36.8%)	633 (41.7%)	1457 (43.3%)	43.6 (11.7%)	243 (17.4%)	614 (19.8%)

5.3 Behavior of wall

Fig. 13 shows the time histories of the flexural rotations of wall in the first story, θ_{w1}, and that of the foundation, $\theta_{footing}$, under the MCE (0.3XY) in comparison with the experimental and analytical results. In the experimental result (distorted model), the angles of rotation at the foundation due to the uplift of the foundation base are considerably larger than those in the first story. In the analytical result of the flexible-base model (true replica model), the flexural rotation in the first story, θ_{w1}, is comparable to that of the experiment, while the flexural rotation of the footing, $\theta_{footing}$, is slightly smaller than the θ_{w1}. The θ_{w1} of the fixed-base model is larger than that of the flexible-base model during table excitation.

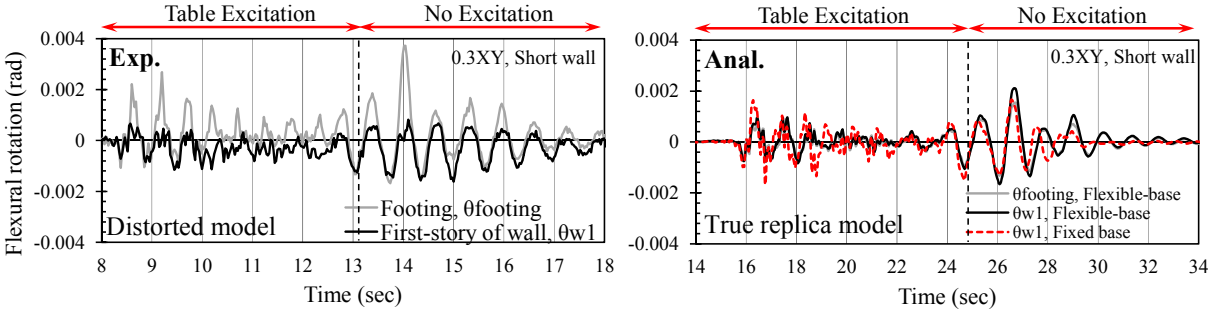

(a) Short wall (left)

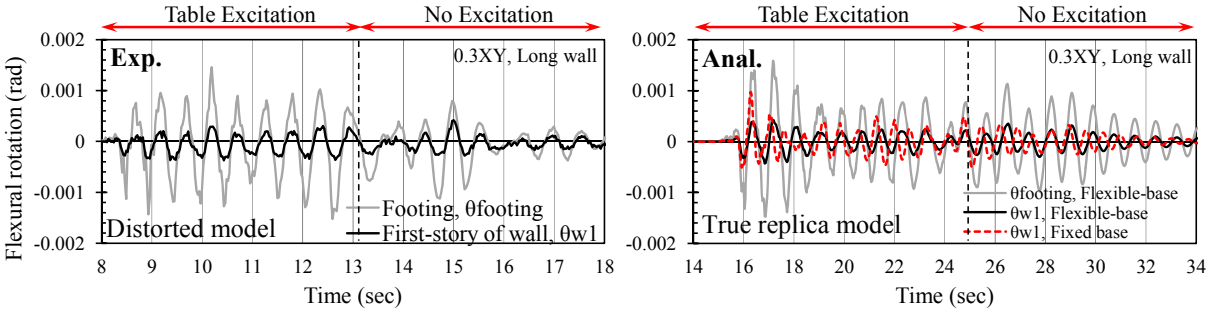

(b) Long wall (left)

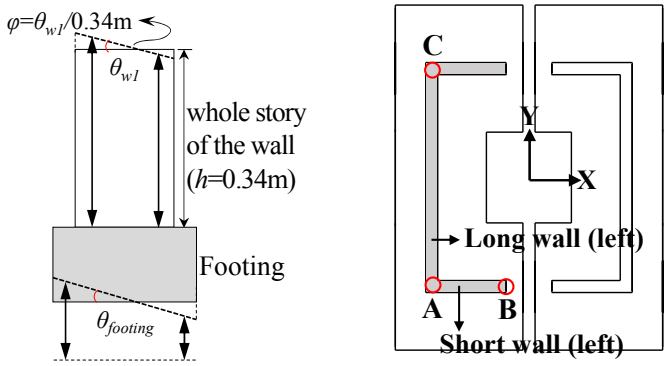

(c) Description of core wall

Fig. 13 Flexural rotation in the core wall under 0.3XY (MCE)

In accordance with the displacement-based design method proposed in ACI 318-05 (2005), special boundary details were imposed on the short wall in the first story with the expected plastic rotation of θ_p = 0.00537 rad (Lee et al. 2015). Fig. 14 shows the moment-curvature curves under the assumption loads of only 1.0 dead load (DL) and DL/3.59. In Fig. 14(a), the ultimate curvature corresponding to a strain of 0.00638 is $\varphi_u = \varepsilon_{cu} / c$ = (0.00638)/(2.36 m) = 0.0027 rad/m for the prototype, with φ_u = 0.041 rad/m for the 1:15-scale model, and the value of curvature for the limiting strain of 0.003 is $\varphi_{cl} = \varepsilon_{cl} / c$ = (0.003)/(2.36 m) = 0.00127 rad/m for the prototype, with φ_{cl} = 0.0191 rad/m for the 1:15-scale model. In the experimental results of the distorted model (DL/3.59), however, under 0.3XY, the maximum value of the measured curvature in the short wall is 0.0085 rad/m, which is only 21% of 0.041 rad/m, the intended ultimate value of curvature in the design phase.

In the analytical results of the true replica model (1.0 DL), the moment and curvature of the fixed-base model (Fig. 14) are larger than those of the flexible-base model with small inelastic energy dissipation, while the wall in the flexible-base model behaves elastically.

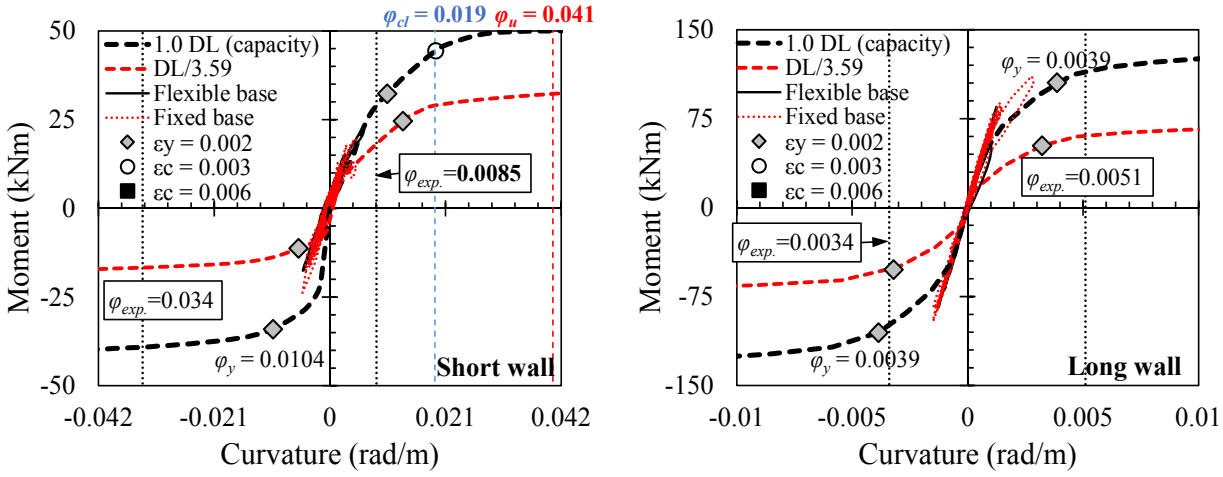

(a) X-dir. (b) Y-dir.

Fig. 14 Relation of the moment and curvature (M-φ) in core wall (Lee et al. 2015)

Fig. 15 shows the axial strain of core wall in the first story at time instants of maximum curvature (ϕ). The axial strains of the core wall in the first story under 0.3XY are within 0.002 m/m. The compressive strain of the edge (Point B in Fig. 13(c)) of the special boundary elements (Fig. 15(a)) is approximately 0.001 m/m, and the corresponding maximum curvature is 0.00621 rad/m and 0.0049 rad/m in the flexible-base and fixed-base models, respectively, during no excitation (Table 3), which is smaller than that of the experimental model (0.0085 rad/m) under DL/3.59, and 10~15% of 0.041 rad/m, the intended ultimate value of curvature in the design phase.

Fig. 16 compares the demand of the relations between axial force and bending moment (P-M) under 0.3XY with the capacity, ϕP-ϕM interaction diagram. The measured axial forces are less than a half and one-third of the maximum capacity in the X and Y directions, respectively. The demand at most of time instants are within the capacity of ϕP-ϕM, while few instants slightly exceed the tensile-controlled limit of the capacity.

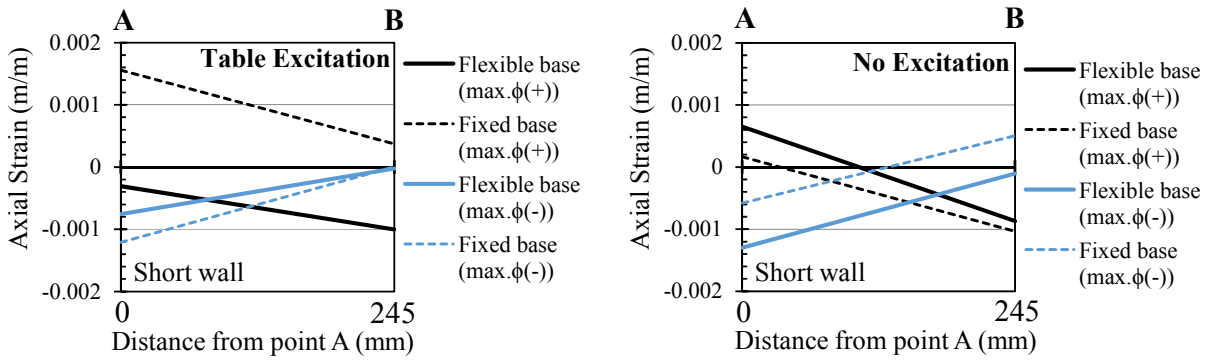

(a) Short wall (left)

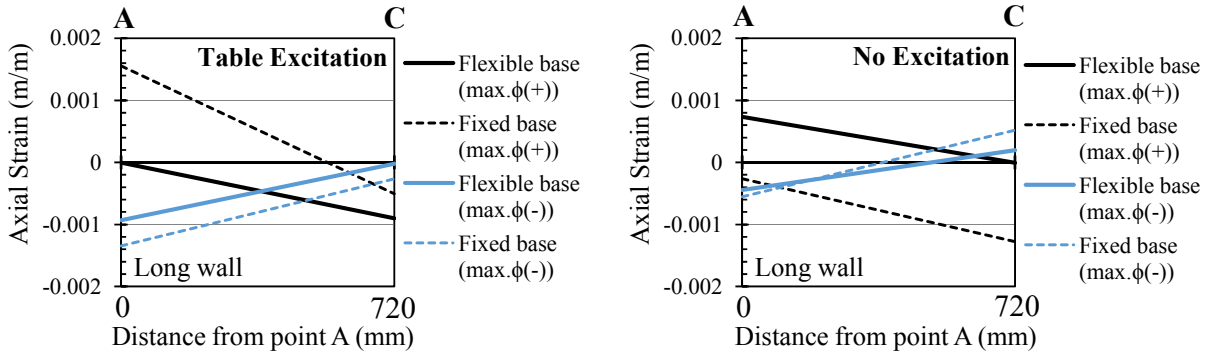

(b) Long wall (left)

Fig. 15 Axial strain of core wall in the first story at time instants of maximum curvature under 0.3XY (MCE, Points A to C in Fig. 13(c))

Table 3. Maximum responses on left core wall in the first story under 0.3XY (MCE)

(a) Left wall in the **X direction** in the first story

Model		Short wall			Moment (kNm)	Shear force (kN)
		Flexural rotation (rad)	Curvature (rad/m)	Compressive Strain* (m/m)		
Flexible base	Table Excitation	0.00102	0.00299	0.00100	15.0	33.6
	No Excitation	0.00211	0.00621	0.00106	22.9	35.9
Fixed base	Table Excitation	0.00168	0.00495	0.00100	23.7	34.8
	No Excitation	0.00167	0.00490	0.00105	19.5	19.7

(b) Left wall in the **Y direction** in the first story

Model		Long wall			Moment (kNm)	Shear force (kN)
		Flexural rotation (rad)	Curvature (rad/m)	Compressive Strain* (m/m)		
Flexible base	Table Excitation	0.00043	0.00126	-0.00103	84.8	42.1
	No Excitation	0.00035	0.00103	-0.00110	56.7	17.2
Fixed base	Table Excitation	0.00097	0.00286	-0.00132	110.8	45.0
	No Excitation	0.00051	0.00149	-0.00137	88.5	28.6

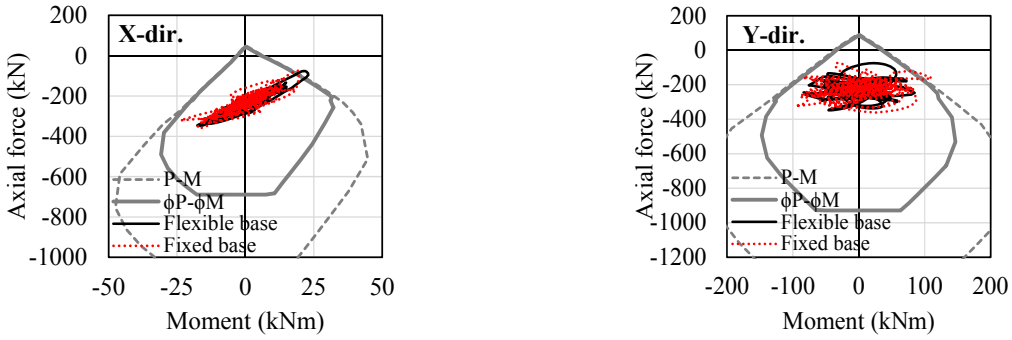

(a) X-dir. (b) Y-dir.

Fig. 16 Hysteretic curves between the axial force and bending moment (*P-M*) in the left core wall under 0.3XY (MCE)

6. CONCLUSIONS

This study investigates seismic responses of an RC high-rise flat-plate core-wall building structural system through the analytical simulation of the shake-table responses of a 1:15 scale 25-story flat-plate core-wall RC residential building model by using the nonlinear analysis program, PERFORM-3D. The following conclusions are drawn from these investigations:

(1) The foundation rocking tends to increase the lateral resistance of the flat-plate frame. In the flexible-base (foundation rocking) model, the base shear contributed by flat-plate frame is approximately 30~40%, whereas over 90% of the story shear is resisted by the core wall in the fixed-base model. The overturning moment (OTM) contributed by the flat-plate frame is approximately 30~50% of the total overturning moment, and similar to the moment due to coupled tension and compression axial forces in the core-wall system. In addition, the ratio of the bending moment of the core-wall to the moment due to tension/compression coupling forces is about 40%:60% (flexible base) and 30%:70% (fixed base).

(2) The energy dissipation through the inelastic deformation was dominant during the free vibration after termination of table excitation rather than during table excitation. The amount of the total dissipated energy in the fixed-base model is 90% of that in the flexible-base model. Under the maximum considered earthquake (MCE) in Korea, the ratio of the amounts of dissipated inelastic energy in the wall : coupling beam : slab in the flexible-base model is about 1:5:4 with that in the fixed-base model being 2:6:2. The fixed-base model increases the dissipated inelastic energy in the wall, while decreasing that in the slab, when compared with the case of the flexible-base model.

(3) Under the MCE in Korea, the base moment and curvature of the core wall in the fixed-base model are larger than those in the flexible-base model with small inelastic energy dissipation, while the wall in the flexible-base model behaves elastically. In addition, the walls with special boundary elements in the first story did not exhibit any significant inelastic behavior with a maximum curvature being only 10~15% of the intended ultimate value of in the design phase, 0.041rad/m.

ACKNOWLEDGMENTS

The research presented herein was supported by the Natural Hazard Mitigation Research Group, Ministry of Public Safety and Security of Korea, through the contract No. MPSS-NH-2013-70. The authors are grateful for this support.

REFERENCES

American Concrete Institute (ACI) (2005). Building code requirements for structural concrete and commentary, *ACI 318-05*.

American Society of Civil Engineers (ASCE) (2014). Seismic evaluation and retrofit of existing buildings. *ASCE/SEI 41-13*, Reston, VA.

Architectural Institute of Korea (AIK) (2009). Korean Building Code. *KBC 2009*. Seoul, Korea. (in Korean)

CSI (2011) *Components and Elements for PERFORM 3D and PERFORM-Collapse Ver. 5*, Computers and Structures Inc., Berkeley, CA.

International Code Council, International Building Code, Country Club Hills, IL, 2006.

Lee, H. S., Hwang, K. R., & Kim, Y. H. (2015). Seismic performance of a 1: 15-scale 25-story RC flat-plate core-wall building model. *Earthquake Engineering & Structural Dynamics*, 44(6), 929-953.

PEER/ATC. Modeling and acceptance criteria for seismic design and analysis of tall buildings. *PEER/ATC 72-1 Report*. Applied Technology Council. Redwood City, C.A., October 2010.